

## Measurement of alkali–silica reaction progression by ultrasonic waves attenuation

François Saint-Pierre, Patrice Rivard\*, Gérard Ballivy

*Centre de Recherche sur les Infrastructures en béton — CRIB, Civil Engineering Department, Université de Sherbrooke, Canada J1K 2R1*

Received 3 October 2005; accepted 22 February 2007

### Abstract

Development of non-destructive methods, developed specifically for assessing the damage induced by alkali–silica reaction (ASR) in concrete structures, is needed in order to carry out a systematic evaluation of the concrete condition. The aim of this study is to monitor the evolution of the ASR-damage in laboratory with concrete samples with ultrasonic pulse velocity and attenuation of ultrasonic waves methods. For this study, results of both methods were compared with expansion and mass variation.

One reactive concrete mixture was made with reactive aggregate, and one other mixture, incorporating non-reactive aggregate, was made as a control. Specimens were kept at 38 °C in a 1 mol l<sup>-1</sup> NaOH solution to accelerate the reaction. Attenuation of transmitted ultrasonic waves appeared to be more appropriate for the evaluation of ASR-damage compared with pulse velocity. The attenuation of accelerated reactive concrete cylinders increased by 90% after 1 year while it increased by 40% for the non-reactive concrete used as a control. Major part of the attenuation increase in the non-reactive concrete is due to liquid absorption.

This work suggests that in-situ non-destructive techniques based on ultrasonic wave attenuation, like ultrasonic attenuation tomography, should be developed in order to evaluate the development of ASR in concrete structures. Petrographic examination confirmed that damage to concrete is associated with ASR.

© 2007 Elsevier Ltd. All rights reserved.

**Keywords:** Alkali–aggregate reaction; Spectral analysis; Expansion; Microcracking; Ultrasound

### 1. Introduction

Alkali–silica reaction (ASR) is a chemical reaction between ions dissolved in the cement pore solution and reactive silica phases in the aggregate particles. This reaction causes swelling and microcracking of the aggregates and the cement paste. Damages are also visible in the concrete structure surface and may take a variety of forms, from typical non-oriented surface cracking known as map-cracking, to highly oriented cracks in zones where concrete is stressed. Resulting damage changes the physical properties of concrete and influences non-destructive measurements.

In order to rehabilitate concrete deteriorated by alkali–silica reaction, or even to determine whether it is needed to repair the

concrete, it is often necessary to carry out a systematic evaluation of the state of the reaction prior to specifying any kind of repair procedure. Efforts are made to develop innovative methods for condition assessment, performance prediction, and maintenance management for the cost-effective rehabilitation of aging and deteriorating concrete structures. These investigative methods should however be adapted to the specific deterioration process affecting structures, such as ASR.

ASR progression has been widely monitored with conventional destructive methods (mechanical testing and petrography on cores drilled in the structures) but there is a lack of information regarding non-destructive evaluation (NDE).

Visual inspection can give an overall estimate of the damage extent but this method remains highly qualitative, superficial, and strongly depends on the inspector experience. Semi-quantitative surface methods have also already been proposed, based on the measurements of the crack width that intersects

\* Corresponding author. Tel.: +1 819 821 8000x63378; fax: +1 819 821 974.  
E-mail address: [Patrice.Rivard@Usherbrooke.ca](mailto:Patrice.Rivard@Usherbrooke.ca) (P. Rivard).

lines drawn on the surface of the assessed structure [1,2]. However, these methods appeared to be less effective [3].

NDE based on ultrasonic methods, mainly the ultrasonic pulse velocity (UPV) method has also been used to assess ASR on drilled cores, on small size sections like bridge pier, as well as on laboratory specimens. However, conclusions were not always consistent since the sensitivity of UPV is not efficient. Several studies reported that UPV, in ASR-affected concrete decreases with expansion [4–11], but others have shown that UPV are slightly affected by ASR, except when the expansion levels are very high [12–14]. For instance, Ahmed et al. [8] observed a loss of 24% after the concrete had reached an expansion level around 0.1%. Bungey [10] observed the same loss of UPV, but this time after an expansion level of 0.2%. The author also measured a decrease of attenuation (loss of stress wave energy) close to 95% at an expansion level of 0.5%.

This paper describes and compares ultrasonic methods and destructive methods used to characterize the ASR evolution in laboratory concrete. Measurements of ultrasonic pulse velocity method, ultrasonic wave attenuation, expansion rate, petrographic analysis, compressive strength, and Young modulus were used to monitor the deterioration of concrete associated with ASR over 52 weeks in accelerated conditions. A comparison between the attenuation of transmitted ultrasonic waves method and the expansion rates values is presented.

## 2. Materials

### 2.1. Aggregates

The Spratt limestone was used in the reactive concrete mixture. This aggregate, well-known for its high reactivity, is a fine-grained siliceous limestone with chalcedony inclusions, quarried near Ottawa (Canada). The Limeridge limestone, quarried from Eastern Township (Canada) and composed of 97% calcite, was used in the control mixture. The fine aggregate in both mixtures is a non-reactive natural sand from the Sherbrooke area (Canada) and consists of quartz and feldspar grains with some metasedimentary particles.

### 2.2. Concrete mixture proportions

Two concrete mixtures were designed with the same proportions (Table 1). The difference is only related to the coarse aggregates type (reactive and non-reactive). Equal mass quantities of coarse aggregate size fraction 5–10, 10–14 mm were used in the concrete. A normal portland cement (0.88%  $\text{Na}_2\text{O}_{\text{eq}}$ ) was used in the preparation of both mixtures. Reagent grade NaOH pellets were added to mixing water to increase the total alkali content of both mixtures to  $5.25 \text{ kg m}^{-3} \text{ Na}_2\text{O}_{\text{eq}}$ .

### 2.3. Casting and conditioning of test specimens

A total of 10 prisms ( $75 \times 75 \times 300 \text{ mm}$ ) with reference stainless steel studs fixed at both ends and 40 cylinders ( $100 \times 200 \text{ mm}$ ) were cast from both mixtures. After 24 h in a curing room, specimens were taken out of the moulds. Reactive (R) and non-

reactive (NR) cylinders, to be used for non-destructive techniques, and prisms used for length variation measurements were soaked into plastic pail filled with  $1 \text{ mol l}^{-1} \text{ NaOH}$  solution. Thirty-two cylinders, to be used for compressive strength, and Young modulus determination, were placed over water in hermetic plastic pails lined with terry clothes, in compliance with the CSA A23.2-14A Canadian Standard. All the pails were stored at  $38^\circ\text{C}$  in a control room. The “zero” length of prisms was set just before immersion into the NaOH solution. The prism expansiveness was monitored regularly during a whole year.

## 3. Test details

### 3.1. Mechanical tests

Mechanical tests were conducted on cylinders to determine the compressive strength and the Young modulus of the concrete in accordance with the ASTM C39M-04a and ASTM C469-02 standards. Tests were performed at 4, 9 and 14 weeks on two samples from each mixture.

### 3.2. Pulse velocity test

This test was used to measure the velocity of an ultrasonic compression wave traveling through the concrete. Measurements were conducted on  $100 \times 200 \text{ mm}$  cylinders with the device shown in Fig. 1, in accordance with the ASTM C597 standard. The device used in this study is composed of two 250 kHz central frequency transducers, a pulse generator, a numerical oscilloscope and a computer with an acquisition system.

The shape of the electrical pulse signal sent to the transmitter transducer is a one period sinusoid with a 250 kHz central frequency and an amplitude of 20 V. The accuracy measured on stress wave travel time measurement is  $\pm 1\%$ .

### 3.3. Attenuation of transmitted ultrasonic waves

The aim of this method is to measure the spectral response of a cylindrical concrete specimen, subjected to an ultrasonic pulse, in order to calculate the loss of spectral gain (i.e. the attenuation). This method is inspired from the spectrum ratio method, which was developed to assess damages related to freezing–thawing cycles [15]. The device used in this study is the same as the one used for the UPV method (Fig. 1). The shape of the electrical pulse signal sent to the transmitter

Table 1  
Mixture proportions

Mixtures	NR (Non-reactive)	R (Reactive)
W/C	0.50	0.50
Coarse aggregates	Limeridge limestone	Spratt limestone
Cement ( $\text{kg m}^{-3}$ )	350	350
Water ( $\text{kg m}^{-3}$ )	175	175
Aggregates ( $\text{kg m}^{-3}$ )	954	954
Sand ( $\text{kg m}^{-3}$ )	946	946
$\text{Na}_2\text{O}_{\text{eq}}$ ( $\text{kg m}^{-3}$ )	5.25	5.25

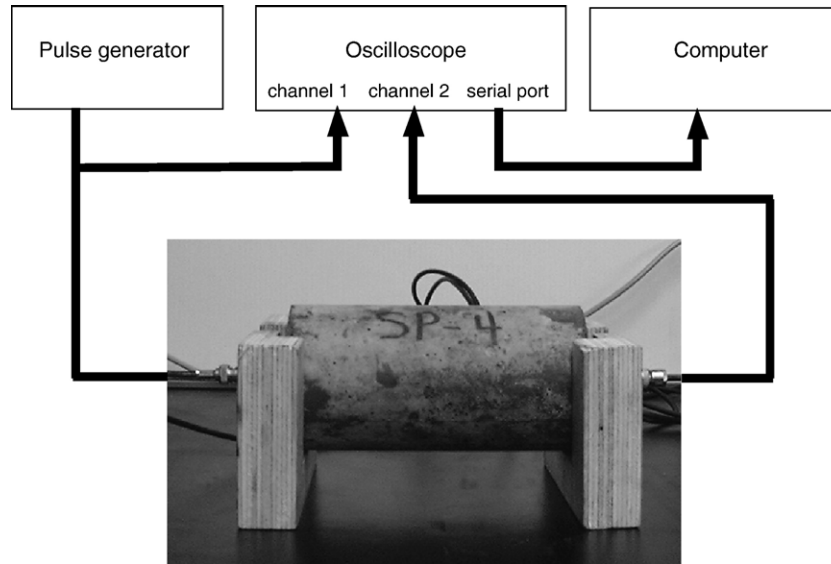


Fig. 1. Device elements for measurement of ultrasonic attenuation.

transducer is a thin rectangle with a  $1 \mu\text{s}$  active time and 20 V of amplitude. Thus, the spectrum of the generator pulse is wider than the transducer spectrum. The sampling rate is 4 MHz and the size of the acquisition windows is set to 0.5 ms. For each measurement, the average was made on 1024 samples in order to reduce signal noises.

The electrical output signal  $y(t)$  of the receiver transducer is influenced by the transducer spectrum, so the output signal spectrum is adjusted with the convolution product between  $y(t)$  and the invert signal function  $y_c(t)$  of the device signature signal. The Fast Fourier Transform (FFT) of this deconvolution integral corresponds to a division in the frequency domain (Eq. (1)) and provides the spectral attenuation of the concrete  $\alpha(f)$ .

$$\alpha(f) = \text{FFT}\left(y(t) * y_c(t)^{-1}\right) = \frac{\text{FFT}(y(t))}{\text{FFT}(y_c(t))} \quad (1)$$

where  $f$  is the frequency.

The value of the attenuation factor  $\alpha$  (a ratio without dimension) decreases when the received amplitude of the electrical signal also decreases. In other words, a decreasing  $\alpha$  factor indicates that the attenuation increases, i.e. that the concrete is deteriorating.

After processing, the results show that the concrete spectral response to an ultrasonic pulse is still noisy, which is mainly due to diffusivity caused by the aggregate diffraction effect [16]. To minimize this effect, four measurements were taken by shifting the specimen in four different positions. Rotations of  $180^\circ$  and sides switching of the specimen were performed between each measurement.

Fig. 2 shows that the concrete behave as a low-pass filter (i.e. signal of the high frequencies signal is strongly attenuated), which can be characterized by a regression line (equation in Fig. 2). This is mainly due to the dissipation caused by the absorption of short wavelengths of the ultrasonic signal by larger aggregate particles.

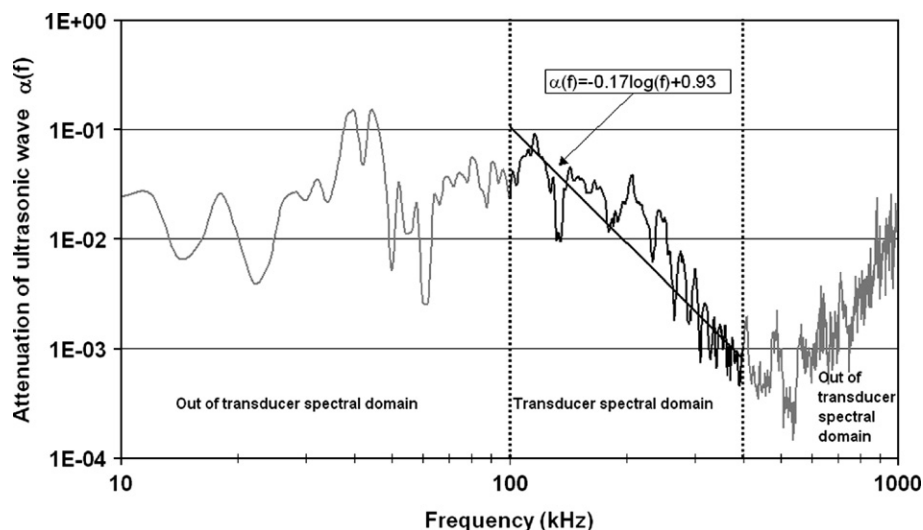


Fig. 2. Four measurements averaging of the concrete spectral response to an ultrasonic pulse.

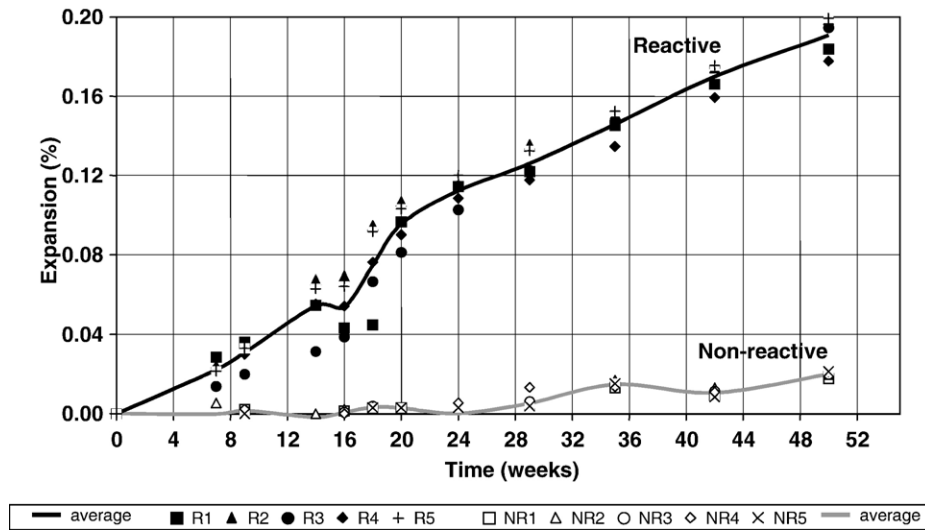


Fig. 3. Expansion of reactive (R) and non-reactive (NR) specimens (38 °C in NaOH solution).

The slope of this line shows some variations because measurements are influenced by the contact between transducers and concrete. However, a previous testing has shown that 100 kHz spectral attenuation, given by the low-pass filter regression line (Fig. 2), was less affected by transducers contact. A corrective equation is used to normalize attenuation to a one-meter length specimen (Eq. (2)) in order to provide results independent from the specimen length.

$$\alpha_n = \frac{\alpha \cdot \ln}{l} \quad (2)$$

$\alpha_n$       attenuation factor normalized  
 $l$         specimen length  
 $\ln$        normalization length (one meter in this study)

All specimens were characterized by the attenuation measurement at a 100 kHz frequency in the spectral response to an ultrasonic pulse and normalized to a standard cylindrical 1 m length specimen. The accuracy of the amplitude measurement, calculated from the standard deviation on several samples, is  $\pm 5\%$ .

### 3.4. Petrographic examination

Concrete specimens were subjected to a petrographic examination at the end of the test program in order to confirm that damage to concrete was mainly associated with ASR. The examination was conducted according to the *Damage Rating Index* method [17,18]. Basically, this method consists of a petrographic examination performed on a polished concrete section with a stereomicroscope at a magnification of 16 $\times$ .

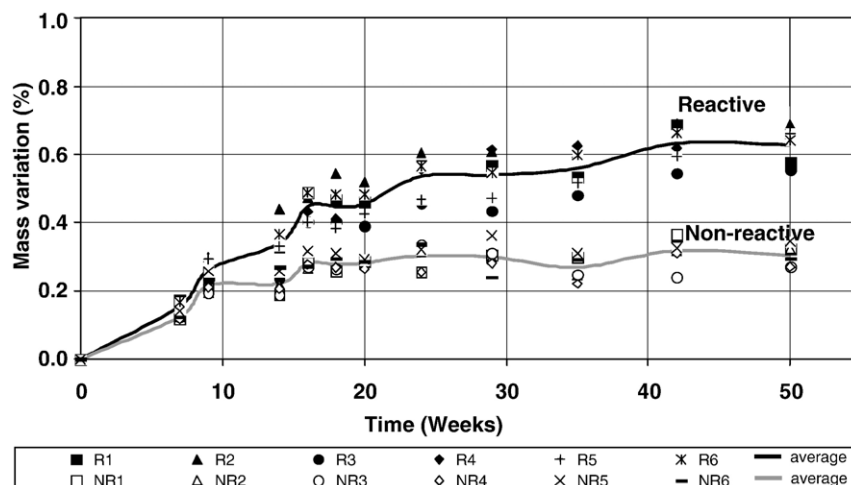


Fig. 4. Mass variation of reactive (R) and non-reactive (NR) specimens (38 °C in NaOH solution).

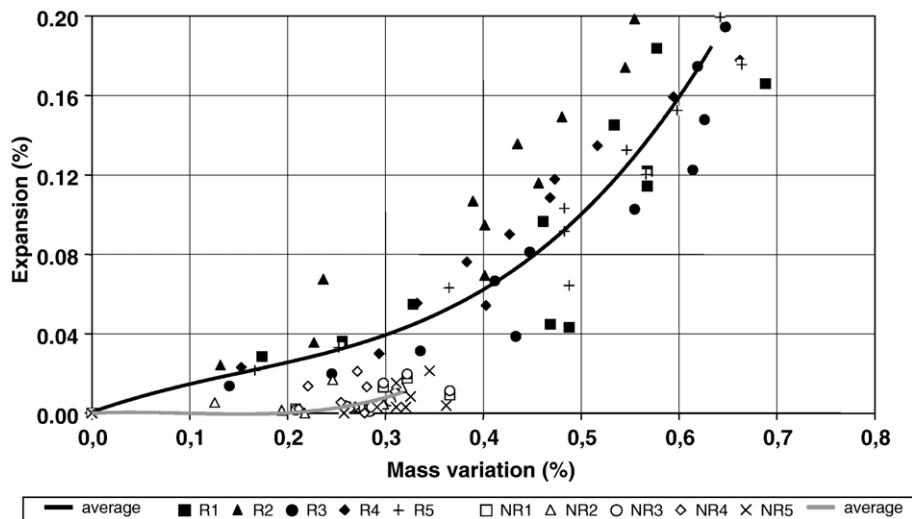


Fig. 5. Comparison between expansion and mass variation of reactive (R) and non-reactive (NR) specimens.

The petrographer identifies and counts selected defects associated with ASR (e.g. cracks in aggregates, reaction rim around aggregates, gel filling air voids, etc.). A DRI number above 30 is considered to be indicative of significant damage.

## 4. Results and discussion

### 4.1. Expansion and mass variation

Mean expansion curves, calculated on five samples from each mixture, are shown in Fig. 3. The reactive mixture (R) shows quite constant expansion while the non-reactive mixture (NR) shows very low expansion. Expansion levels at 50 weeks are 0.20% for the R mixture and 0.02% for the NR mixture.

Fig. 4 shows that the mass of test specimens quickly increases due to liquid absorption after being soaked into the  $1 \text{ mol l}^{-1}$  NaOH solution. The mass variation curves for the NR mixture stabilized after 10 weeks. It can be observed that ASR increases the rate of liquid uptake due to the formation and

swelling of the reaction gel. The mass of the reactive mixture is still increasing after 10 weeks (about 0.05% per 10 weeks).

Mass variation is compared with the expansion of prisms. Fig. 5 shows that the NR variation mass does not step over 0.3% whereas the R variation mass increases in two parts. The first part is a fast increase (0.075% of mass variation for 0.01% expansion level) and is due to ASR and immersion absorption. The second part occurs after 0.05% of swelling and is caused by water absorption with forming gel (0.02% of mass variation for 0.01% expansion level).

Fig. 5 also shows that the mass variation of NR specimens is due to liquid absorption after being soaked into NaOH solution, and does not have a significant effect on the expansion.

### 4.2. Mechanical tests

The evolution of the compressive strength, calculated from two samples from each mixture, is shown in Fig. 6. The compressive strength of the R mixture and the NR mixture

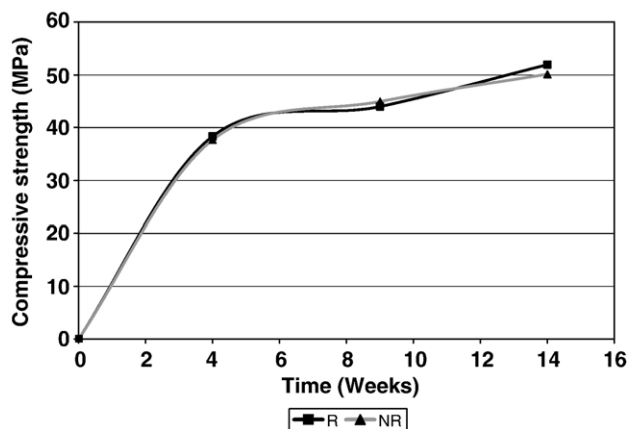


Fig. 6. Compressive strength evolution of reactive (R) and non-reactive (NR) specimens (38 °C over water).

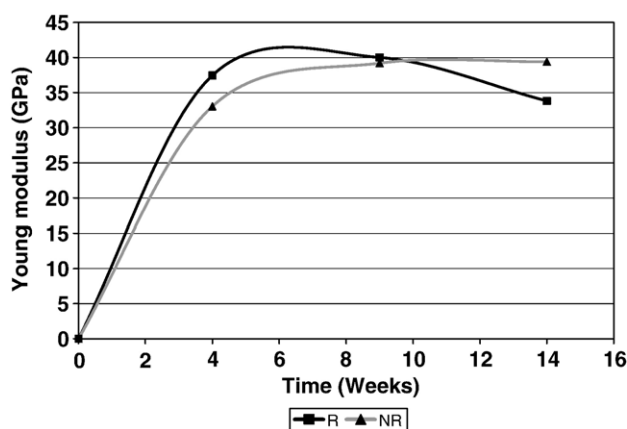


Fig. 7. Young modulus evolution of reactive (R) and non-reactive (NR) specimens (38 °C over water).

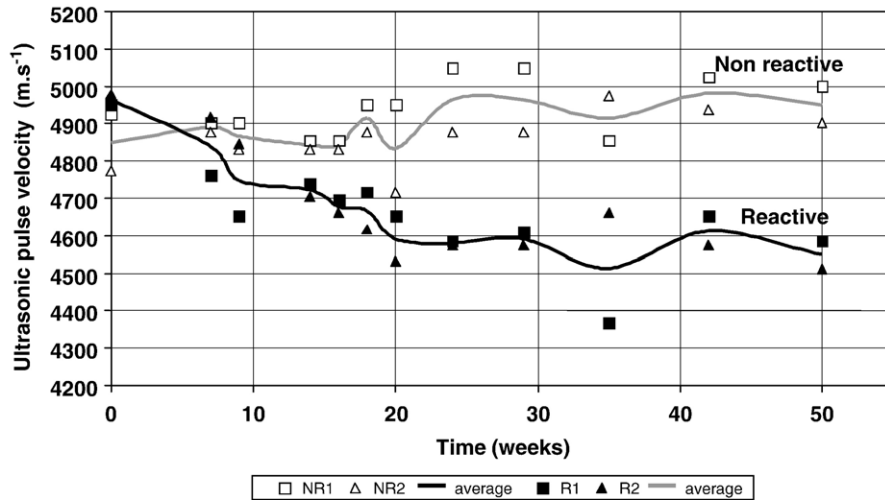


Fig. 8. Ultrasonic pulse velocity of reactive (R) and non-reactive (NR) specimens.

increases. Both reactive mixtures follow a flat trend after reaching maximal strength at 4 weeks. Thus, ASR did not affect the compressive strength during this period. However, recall that the specimens were kept over water, and that ASR development is slower in this environment compared with NaOH solution immersion.

Fig. 7 shows that the Young modulus is more sensitive to ASR than the compressive strength is, which agrees with literature [4,5,8,9,12,13]. The NR mixture shows a very slight increase after 4 weeks whereas the value decreases at 14 weeks for the R mixture. This decrease indicates that the stiffness of the concrete is reduced, and this has an influence on the physical properties measured with non-destructive techniques such as UPV or ultrasonic wave attenuation.

#### 4.3. Ultrasonic pulse velocity test

Fig. 8 shows the evolution of the ultrasonic pulse velocity of both mixtures. The velocity of all specimens was lying between

4400  $\text{m s}^{-1}$  and 5100  $\text{m s}^{-1}$ . These velocities are considered to be high and are usually found on good quality concrete (ASTM C597 standard).

The pulse velocity of the NR mixture increased by 2.0% during 1 year, whereas the R mixture pulse velocity decreased by 8.0% during the same period of time. This increase observed with NR mixture is related to the increase of compressive strength with time caused by ultimate strength late-adding cement phase due to  $\text{C}_2\text{S}$  hydration phenomenon. One can note that, for both mixtures, velocities seem to reach a flat trend, which does not enable anyone to differentiate the R mixture from the NR mixture after 20 weeks.

The expansion can be compared with the ultrasonic pulse velocity variation. Fig. 9 shows that the UPV variation is close to 4.0% for an expansion level of 0.03% and reaches 8.0% when the expansion level is higher than 0.09%. It means that although the expansion of prism specimens increases, the pulse velocities do not step over 8.0%, and follow a flat trend after an expansion higher than 0.09%.

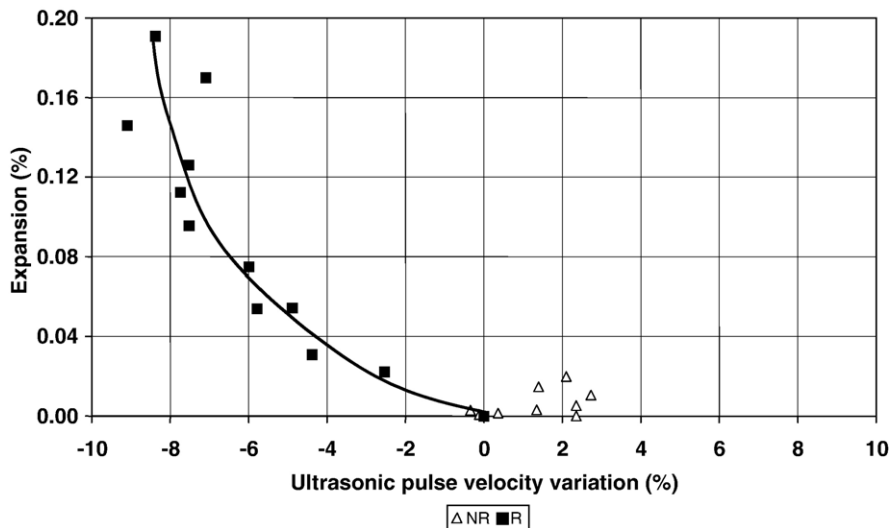


Fig. 9. Comparison between expansion and ultrasonic pulse velocity.



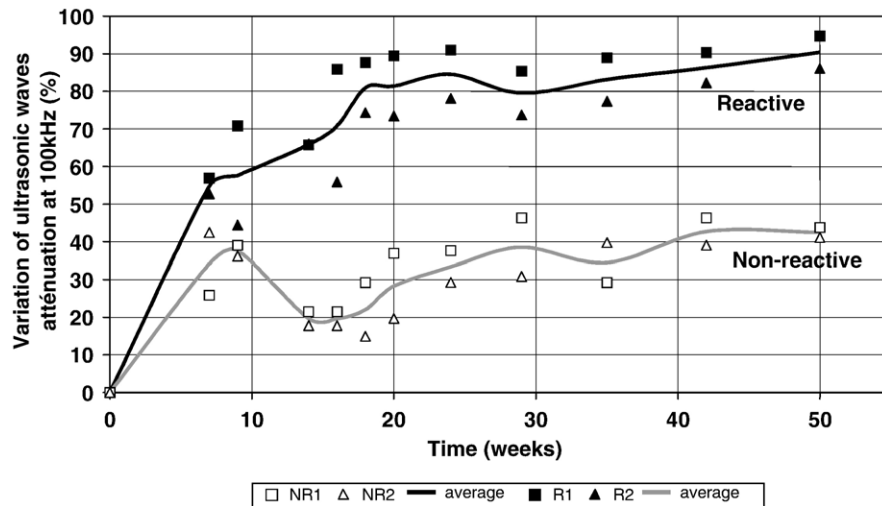


Fig. 10. Ultrasonic waves attenuation variation of reactive (R) and non-reactive (NR) specimens.

#### 4.4. Attenuation of transmitted ultrasonic waves

Attenuation in ASR-affected concrete is mainly associated with two phenomena: the first is called diffusivity and is caused by wave multiple diffractions on ASR-damages, such as cracks and gel whereas the second phenomenon is called dissipation and is caused by the change of concrete inelasticity matrix due to ASR. Dissipation can also be due to inter-grain friction [19]. ASR leads to changes at the aggregates periphery (development of reaction rims, debonding, accretion of silica gel...) so the dissipation is meant to increase. Furthermore, if the diameters of the aggregates change because of the ASR, the total attenuation coefficient, which depends mainly of the wavelength and frequency, is affected [20].

After 50 weeks, the signal received from the R mixture becomes nearly flat (indicating strong attenuation of all waves)

whereas the signal from the NR mixture does not appear to be affected over the 50 weeks. Fig. 10 shows the variation of the attenuation factor measured on two samples from each mixture during 50 weeks in NaOH solution. A mean attenuation factor of 0.045 is calculated after 50 weeks for the R mixture, which corresponds to a total attenuation increase of 90% (Fig. 10). After the same period, the NR mixture shows a mean attenuation factor of 0.08, corresponding to an attenuation increase of 30%. The attenuation is still increasing for the R mixture while it tends to remain constant for the NR mixture.

It has been observed (Section 4.1 and Fig. 4) that the mass of specimens increases due to the absorption of liquid (immersion into NaOH solution). This phenomenon can also be observed in Fig. 10. The attenuation variation curve of the NR mixture shows that the attenuation variation due to the immersion of specimen is about 30%. Considering this value to be suitable for

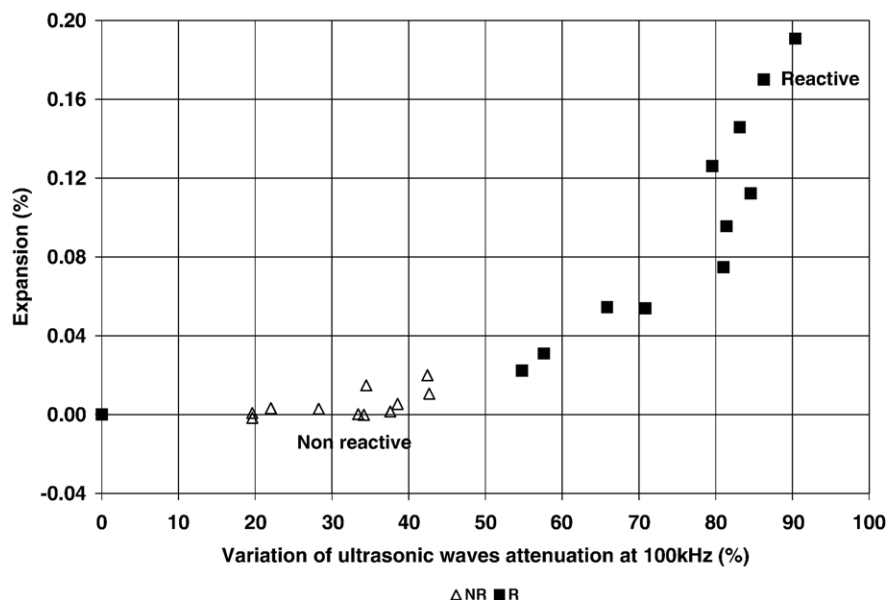


Fig. 11. Comparison between expansion and ultrasonic waves attenuation variation of reactive (R) and non-reactive (NR) specimens.

the R mixture, one may infer that ASR caused an attenuation of about 60% after 50 weeks in NaOH.

The mean curves of both mixtures are rising and falling quite significantly between 9 and 20 weeks (Fig. 10). As seen in Fig. 4, this period also corresponds to a disturbing mass variation at the end of the liquid absorption period (about 18 weeks). Thus, disturbing mass variation causes variations of the physical properties of concrete that also have an effect on ultrasonic wave attenuation variations.

Comparison between the expansion and the variation of ultrasonic wave attenuation at the frequency of 100 kHz is shown in Fig. 11. The attenuation variation of the R mixture reaches about 90% when the expansion level is higher than 0.1%. This kind of information is relevant for an ASR monitoring program based on measurements conducted on cores drilled from different members of an affected structure. The results would then be valuable to estimate the expansion level and degree of damage to concrete.

#### 4.5. Petrographic examination

Two polished samples prepared from each mixture were observed under the stereomicroscope. The petrographic examination confirmed that the non-reactive mixture did not suffer from ASR as well as confirming that damage to concrete is very high in the reactive mixture.

The DRI method yields a mean value of 14 for NR mixture. Closed cracks in coarse aggregates essentially contributed to this number but are not necessarily associated with ASR. Crushed aggregates usually exhibit cracks due to quarrying operations [18]. No cracks were observed in the cement paste.

Values ranging from 505 to 555 were obtained for the R mixture. These values are very high and are typical of severely ASR-damaged concrete. Several cracks filled with gel were observed in the coarse aggregates and in the cement paste. Gel was also observed lining or filling air voids.

## 5. Conclusion

The evolution of the ASR on concrete specimens was monitored with two methods: ultrasonic pulse velocity and attenuation of transmitted ultrasonic waves. It was shown that the sensitivity of pulse velocity method is too low to establish damage criteria associated with ASR. Virtually no variation was observed after 20 weeks in NaOH on both reactive and non-reactive mixtures whereas the attenuation increased quickly with the concrete expansion. For instance, the pulse velocity measured on the reactive mixture after 50 weeks decreased by about 8% whereas the attenuation variation associated only with ASR was close to 60%. Laboratory tests suggest that the 100 kHz attenuation, normalized to a 1-meter length concrete cylinder, is an effective parameter to monitor ASR, although the variability observed in this study would make it semi-quantitative (e.g. no damage, very low damage, low damage, etc...).

Methods based on the attenuation of stress waves rather than velocities should be used to assess in-situ ASR-affected

concrete structure. For instance, systematic core drilling and attenuation measurements should be integrated into any maintenance program of a structure suffering from ASR. A ranking of the damage extent would then be carried out. When combined with other evaluation techniques, such as mechanical properties assessment or petrographic examination, valuable information should be available in order to assess the extent and progression of the deleterious reaction, and ultimately to forecast the residual expansion.

## Acknowledgments

GRAI (Groupe de Recherche sur l'Auscultation et l'Instrumentation) technical staff is acknowledged. Financial support has been provided by the NSERC (Natural Sciences and Engineering Research Council of Canada) by the FQRNT (Fonds Québécois de Recherche sur la Nature et les Technologies) and by the CRIB (Centre de Recherche sur les Infrastructures en Béton).

## References

- [1] ISE, Structural Effects of Alkali-Silica Reaction: Technical Guidance on the Appraisal of Existing Structures, The Institution of Structural Engineers (ISE), London, UK, 1992.
- [2] LCPC, Détermination de l'indice de fissuration d'un parement de béton, Méthode d'essai LCP, vol. 47, Laboratoire central des ponts et chaussées, Paris, France, 1997.
- [3] N. Smaoui, M.A. Bérubé, B. Fournier, B. Bissonnette, B. Durand, Evaluation of the expansion attained to date by concrete affected by alkali-silica reaction. Part 1: Experimental study, Canadian Journal of Civil Engineering 31 (2004) 826–845.
- [4] R.N. Swamy, M.M. Al-Asali, Engineering properties of concrete affected by alkali-silica reaction, ACI Materials Journal 85 (5) (1988) 367–374.
- [5] J.L. Gallias, Comparison of damaging criteria for testing aggregates by autoclaving treatment, in: R. Bérubé, B. Fournier, B. Durant (Eds.), Proc. of the 11th ICAAR, Québec City, Canada, 2000, pp. 949–958.
- [6] T. Kojima, H. Hayashi, M. Kawamura, K. Kuzume, Maintenance of highway affected by AAR, in: R. Bérubé, B. Fournier, B. Durant (Eds.), Proc. of the 11th ICAAR, Québec City, Canada, 2000, pp. 1159–1166.
- [7] K. Ono, M. Taguchi, Long-term behavior of AAR bridge pier and the internal deterioration, in: R. Bérubé, B. Fournier, B. Durant (Eds.), Proc. of the 11th ICAAR, Québec City, Canada, 2000, pp. 1167–1174.
- [8] T. Ahmed, E. Burley, S. Rigden, A. Abu-Tair, The effect of alkali reaction on the mechanical properties of concrete, Construction and Building Materials 17 (2) (2002) 123–144.
- [9] L.J. Monette, N.J. Gardner, P.E. Grattan-Bellew, Residual strength of reinforced concrete beams damaged by alkali-silica reaction — examination of damage rating index method, ACI Materials Journal 99 (1) (2002) 42–50.
- [10] J. Bungey, Ultrasonic testing to identify alkali-silica reaction in concrete, British Journal Of Non-Destructive Testing 33 (5) (1991) 227–231.
- [11] B. Fournier, M.A. Bérubé, Alkali-aggregate reaction in concrete: a review of basic concepts and engineering implications, Canadian Journal of Civil Engineering 27 (2000) 167–191.
- [12] D.W. Hobbs, Some tests on fourteen year old concrete affected by the alkali-silica reaction, in: Noyes Publications (New Jersey USA) (Eds.), Proc. of the 7th ICAAR, Ottawa, Canada, 1986, pp. 342–346.
- [13] R. Pleau, M-A. Bérubé, M. Pigeon, B. Fournier, S. Raphaël, Mechanical behaviour of concrete affected by ASR, in: Elsevier Applied Science (England) (Eds.), Proc. of the 8th ICAAR, Kyoto, Japan, 1989, pp. 721–726.
- [14] S. Amasaki, N. Takagi, The estimate for deterioration due to alkali-silica reaction by ultrasonic spectroscopy, in: R. Bérubé, B. Fournier, B. Durant (Eds.), Proc. of the 8th ICAAR, Kyoto, Japan, 1989, pp. 839–844.



- [15] M.N. Toksöz, D.H. Johnson, A. Timur, Attenuation of seismic waves in dry and saturated rocks: laboratory measurements, *Geophysics* 44 (4) (1979) 681–690.
- [16] P. Anugonda, J.S. Wiehn, J.A. Turner, Diffusion of ultrasound in concrete, *Ultrasonics* 39 (2001) 429–435.
- [17] P.E. Grattan-Bellew, Laboratory evaluation of alkali–silica reaction in concrete from Saunders Generating station, *ACI Materials Journal* 92 (2) (1995) 126–134.
- [18] P. Rivard, G. Ballivy, Assessment of the expansion related to alkali–silica reaction by the damage rating index method, *Construction and Building Materials* 19 (2) (2005) 83–90.
- [19] Y.H. Kim, S. Lee, H.C. Kim, Attenuation and dispersion of elastic waves in multi-phase materials, *Journal of Physics. D, Applied Physics* 24 (10) (1991) 1722–1728.
- [20] P.A. Gaydecki, F.M. Burdekin, W. Damaj, D.G. John, P.A. Payne, The propagation and attenuation of medium ultrasonic waves in concrete: a signal analytical approach, *Measurement Science & Technology* 3 (1992) 126–134.